Adhesion testing of coated surfaces

Programme of Scientific Support
To Standardisation

Stage II

Final report

PRIME MINISTER'S
SERVICES
SCIENTIFIC,
TECHNICAL AND
CULTURAL AFFAIRS

Table of contents

0 SUMMARY

Surface engineering is a generic technology and is used in a wide range of applications in all industrial sectors including the aerospace, automotive, engineering, construction, biomedical, textile, optical and microelectronics industries. Advanced surface coatings add physical properties, such as lubricity, hardness, or corrosion resistance, to lower-valued substrates that improve the overall quality of the component. In many cases there is a synergetic combination of the properties of the bulk material and the coating. For example, hard coatings on tough substrates are less vulnerable to catastrophic failures than hard bulk materials.

Coating technology is fundamentally dependent upon good adhesion between the coating and the substrate, and in many cases adhesion is the limiting factor for the wider application of the technology. The OSTC project Adhesion testing of Coated Surfaces addresses at this key aspect of coatings. Various engineering methods are used to measure the adhesion. Other methods which are able to quantify the adhesion more directly are being developed. An urgent need to make adhesion values interchangeable between companies is felt. The first step towards this objective is a thorough understanding of the test methods and a clear definition of their validity and limitations. The second step is the standardisation of the tests, which makes an objective and universally accepted quality assurance of the adhesion of coatings possible.

Four adhesion test methods were examined in this project. The scratch test is an egineering adhesion test method which consists of drawing a diamond stylus across the surface under increasing normal load, either stepwise or continuously, until coating spallation failure events are observed in the scratch track. The normal load at which this failure occurs is called the critical normal load L_c (unit: N). This *scratch adhesion test* can be operated in 3 different modes. The first mode is the conventional way of applying the scratch test, i.e. an increasing load with specified ramp is applied on the scratch stylus while the specimen is moved underneath it. This is the "*single pass scratch test (SPST)*". The position along the scratch track where this failure event is produced is evaluated by optical microscopy, and the corresponding normal load can easily be calculated from the test conditions. This load Lc is related to the adhesion of the coating. In the second mode, i.e. the "*constant load scratch test (CLST)*", separate scratches are made at a constant load, and the load is increased between successive scratches. Again, the load provoking failure is defined as the critical load L_c. In the "*multipass scratch test (MPST) "* mode the specimen is subjected to repeated scratching under a constant sub-critical load within the same scratch track. The number of passes at which the first failure event appears is then the criterion for adhesion.

The second adhesion test method is the *Rockwell indentation test*. This method has an even more simple concept than the scratch tests and can be performed with a Rockwell hardness tester. An indent is made in the material and the nature of the damage of the coating nearby the indent is evaluated microscopically using predefined failure classes.

A more direct measurement of the adhesion is offered by the *four point bending adhesion test*. A crack is initiated between the coating and the substrate, e.g. by chemical dissolution of the interface. A shear stress is now imposed at the interface by a four point bending test. At the moment the crack is propagating, the total energy to sustain the shear starts to decrease. This energy release is a direct measure of the adhesion.

The last adhesion test method makes use of a tensile test, i.e the *tensile crack spacing test.* The coated sample is subjected to an increasing tensile strain, causing the film to crack and break into segments. The maximal shear stress at the interface, which is assumed to be related with the adhesion of the coating, can be calculated from the film tensile strength, the coating thickness and the crack spacing distribution. If the crack spacing distribution is scattered, the average value of the spacing is more appropriate. Situations where delamination at the interface occurs can also be taken into account. In the latter case, the energy release rate for film decohesion may be evaluated. It is evident that the coating has to be significantly more fragile than the substrate in order to induce cracking in the coating.

These four adhesion test methods were explored in this project. Parameters of the test set-ups were changed to evaluated the sensitivity of the method to these test parameters. In addition, different coating-substrate systems with different properties were used. This work has led to the evaluation of the applicability of the different test methods and the reliability of the results.

The **selected coatings** were PACVD DLC on C60 steel, PVD TiN on ASP23 steel and electrodeposited Zn on automotive steel. Two different types of each coating were produced with the aim of varying the adhesion, and a third coating with different properties but good adhesion to study the effect of coating intrinsic properties on the result. The *DLC coatings* are known for their good sliding wear resistance. The adhesion on the steel substrate is assured by an a-$Si_{1-x}C_x$:H interlayer. The carbon content in that interlayer is a parameter governing the adhesion. A poorer adhering coating has been deposited by increasing the C content in the interlayer. A third variant of the DLC coatings was produced at a lower bias voltage, yielding a more polymer-like (soft) top coating.

TiN coatings are hard and brittle, frequently used in machining tools to enhance the life cycle. They are deposited at 450°C. A Ti interlayer is needed for the adhesion of the coating on the steel. The bias voltage during the deposition of that interlayer was changed for making a less adhering coating. A third variant of the coating was deposited at a lower temperature (200°C).

The *electrodeposited Zn coating* is mainly used for corrosion protection of steel products. A badly adherent coating was produced by first growing an oxide layer on the steel substrate in a $FeCl_3$ solution. A third variant was deposited at a higher current density in the eletrolytic cell, namely 100 A/dm² instead of the normally used 75 A/dm² for this kind of coating.

A thorough **characterisation** of the obtained coatings was necessary in order to get a better understanding of the results of the different adhesion test methods.

The *thickness* of the coatings was measured by the crater grinding or Calo test. Typical values for the DLC coatings are between 1.5 and 2.5 μm, for the TiN coatings between 2.5 and 4 μm and for the Zn coatings between 40 and 50 μm.

The *surface roughness* of the coated samples was examined by contact profilometry. The measurements were repeated by the three research partners and can be considered as a limited round robin test. When the same tip radius was used (5 μm), the results were within the margin of error. One partner used a larger tip (radius 12.5 μm) which logically resulted in systematically lower surface roughness values.

The *hardness of the coating* and its elastic modulus were measured by nanoindentation. This is a hardness indentation technique which is restricted to the first few hundred nanometers of the material surface to avoid the influence of the substrate. The load and displacement are recorded during the measurement. The results of the nanoindentation confirmed that the TiN are hard and stiff coatings. The obtained values on the DLC coatings gave an expected, but remarkable insight in the differences between the variants. The polymer-like type has only one fourth of the hardness of the other variants. The Zn coatings are soft and showed creep during the indentation test.

The *internal stress state* of the coatings was examined by three different methods. Two of them are based on X-ray diffraction, namely the classical d-sin$^2\psi$ technique and the novel LIBAD (low incident beam angle technique) which is developed especially for thin coatings. The third technique is the bending beam stress measurement, a mechanical method in which the deflection of a glass strip is measured after coating it. The three techniques were used on the TiN coatings. The resemblance of the results by the different methods was good, on the condition that the elastic modulus measured by the nanoindentation was used. The intrinsic stress in the TiN coatings peaks at nearly –5 GPa compressive stress. The internal stress in the DLC could only be measured by the mechanical method since the coating is amorphous and does not produce X-ray diffraction peaks. The stress is also compressive and amounts to –2 GPa. The internal stress in the polymer-like variant is half as high. Finally, the internal stress in the Zn coating was only measured with the d-sin$^2\psi$ method. Here, the stress is rather low and only a few tens of MPa is reached. If higher stresses were build up during the deposition, they are levelled out by creep in the coating.

Further characterisation of the coatings has been done on the *composition* by EPMA and AES, and on the *morphology* by SEM and OM. The conclusions drawn from these investigations are mainly confirming the differences in interface layer for the poor adherent DLC and TiN coating. It also results from Raman measurements that the third variant of the DLC coatings is indeed polymer like.

The characterisation of the used coatings has created a solid base for the evaluation and understanding of the results obtained by the different adhesion test methods. Hereafter, these adhesion tests and their particularities are discussed one by one.

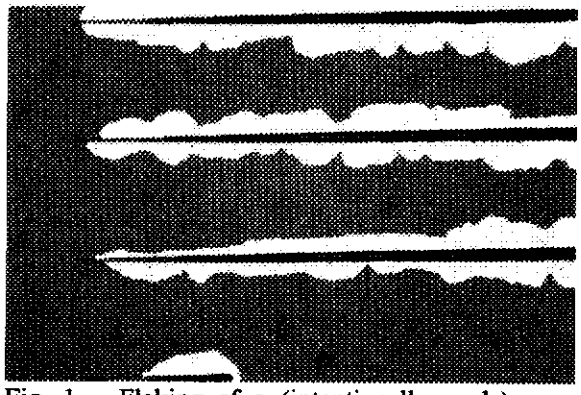

Fig. 1 Flaking of a (intentionally made) poor adherent DLC coating along a scratch track.

The **single pass scratch test** is used classically as an engineering method to assess the adhesion. The test results clearly learn us that the critical load L_c may not be considered as stand-alone criterion of the adhesion. Although the good and poor adhering DLC coating show the same L_c, the failure at L_c is of a completely different nature: the good adherent variant exhibits spallation within the scratch track, while gross flaking in and around the scratch track is produced in the other specimen (fig. 1), which clearly demonstrates the poorer adhesion of the latter. The modified DLC coating (the polymer-like) has a considerably higher L_c. This correlates with its lower internal stress and hardness value.

For the TiN variants as well, no significant difference in critical load value for the good and poor adherent variants could be measured using the single pass progressive load mode scratch test. Moreover, the failure mode and magnitude of the failure events are virtually the same. Both TiN variants spall at the border of the scratch track, exposing the substrate surface. The third variant showed a quite different 'buckling type' failure event and hence, its critical load value cannot be directly compared to those of the other variants.

When using the scratch test on the Zn coating, a perforation of the coating was obtained without any failure mode related to the adhesion. The stylus is ploughing through the coating material. The scratch test method thus can not be used to characterise the adhesion properties of conventional ductile electro-deposited Zn coatings.

The **CLST mode** scratch test enabled to better discriminate between the good and poor adherent DLC and TiN coatings. Higher values of L_c were found for the good adherent DLC coating than obtained by the SPST. It was proven by acoustic emission and frictional force measurements that failure starts in the progressive load mode at a higher load (further away of the beginning of the track) than observed afterwards by optical microscopy. This indicates that the increasing load can induce spallation of delaminated parts of the coating behind the scratch stylus. In other words, a spallation event may be running backwards in the direction of the start of the scratch track at a certain load. We can conclude that the CLST method is more reliable and more sensitive to discriminate coatings on the basis of adhesion. Unfortunately, this method is also more time consuming.

The **multipass scratch test** is even more time- and effort consuming. More information is gained by this test about the toughness and fatigue resistance of the coatings. Due the the excellent toughness properties of the DLC coatings, no coating failure was induced in this mode at a slightly lower load than the Lc obtained by the CLST. The brittle TiN on the other hand showed progressive damaging during the MPST. It was possible to discriminate between the good and poor adherent TiN coatings based by the number of passes before regular spallation failure is observed.

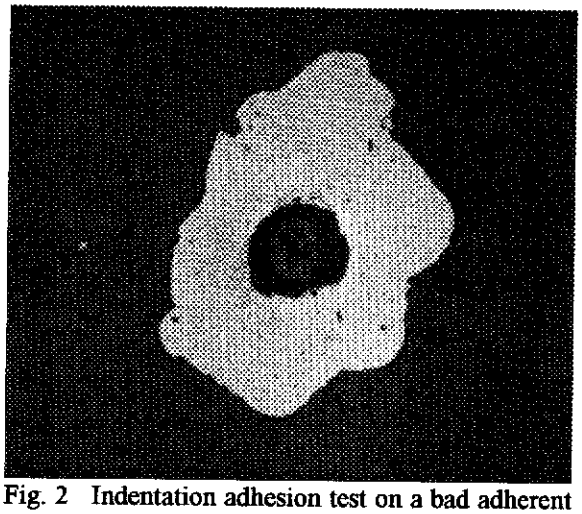

Fig. 2 Indentation adhesion test on a bad adherent DLC coating. A spallation occured around the indent.

The results of the **indentation adhesion test** are in general parallel to those of the scratch test. The test parameters under investigation were the indentation speed, the hold time after indentation and the indentation load. No significantly influence on the results by varying the two first parameters could be found. The failure event became more pronounced with increasing load. On the other hand, there was no transition from one failure mode to another while changing the load. TiN coatings crack at the edge of the indents, while all DLC coatings flakes off upon indentation. Discrimination of the good and poor adherent DLC coatings was only possible when the extent of the spallation, and not only the failure mode in itself, is considered. No spallation nor cracking could be provoked in the soft and ductile Zn coatings, hence this method can not be used to assess the adhesion properties of soft coatings. In general, we can conclude that less information is obtained by the indentation adhesion test than by the scratch test although subsequent indents at increasing normal loads would be a valuable alternative for the latter.

For DLC and Zn coatings the **four point bending technique** is implemented with success. The method gives a direct measure of the strength of the coating-substrate interface. However, the method is complicated and requires careful sample preparation. The test is only applicable if a precrack at the interface can be generated in situ. For the DLC an appropriate method based on the selective dissolution of the interface in a concentrated KOH solution was found. However, it was impossible to initiate crack propagation at the TiN-substrate interface, hence the method could not be applied on the TiN coatings. The numerical test results of the Zn and DLC coatings were as expected, except for the polymer-like DLC in which a different failure mechanism governed the crack propagation.

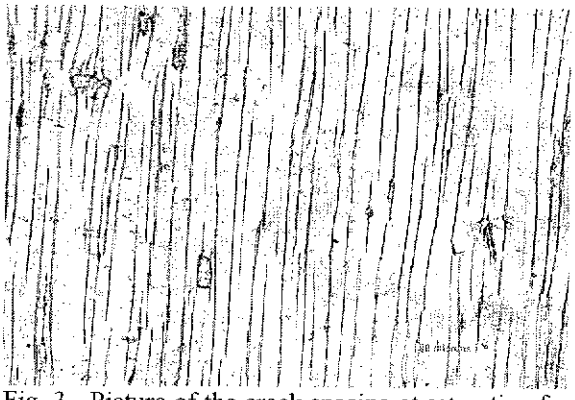

Fig. 3 Picture of the crack spacing at saturation for the good adherent DLC coating on automotive steel (taken by optical microscopy).

The last examined adhesion test method is the **tensile crack spacing technique**. The method showed its applicability for brittle coatings on ductile substrates. Qualitatively, the results for the TiN and DLC coatings (see fig. 3) were as expected, except for the poor adherent DLC coating where spallation occurred. The test can not be used for the ductile Zn coatings.

Different models exist to obtain the maximum interfacial shear strength from the film thickness. Their implementation does not change the qualitative ranking of the coatings, but the absolute values can differ by a factor 3. However, numerous remarks can be made on the relative values of τ_I obtained in the tensile adhesion test. Delamination of the coating is not always obvious when it occurs during the test, unless the coating really flakes off from the substrate. Scanning acoustic microscopy could be used to verify eventual delamination. If the measured (macro-)stress in the DLC coatings is taken into account, the absolute value of the good adherent DLC variants are closer to each other. In the case of TiN, the internal stress (IS) measured by XRD is taken into account. However, the situation here is much more complicated. Internal stresses measured by XRD correspond to the local stress, i.e. the sum of the macrostress and micro- or intrinsic stress is obtained. Only the macrostress is relaxed upon cracking of the coating. In this work, no distinction was made between micro- and macrostress.

The numerical results of the different adhesion test are summarised in the following table:

Technique	Scratch Test SPST	Scratch Test CLST	Scratch Test MPST	Indentation Test	Crack Propagation Test	Crack Spacing Test
coating	L_c [N]	L_c [N]	number of passes	class	G_c [J/m²]	τ_I [Gpa]
DLC A	7.6	12	-	6	523	1.33
DLC B	8.6	8	-	6	24	(1.35)
DLC C	19.8	15	-	no failure	112	0.84
TiN A	78.8	80	15 passes	1	-	2.23
TiN B	74.4	60	10 passes	1	-	2.46
TiN C	76.4	64	15 passes	1	-	0.86
Zn A	-	-	-	-	233	-
Zn B	-	-	-	-	82	-
Zn C	-	-	-	-	168	-

The knowledge and better understanding gained by this work of different adhesion tests has led to the redaction of an improved pre-Standard ENV 1071-3 on the scratch test, the preparation of a pre-standard (ENV) concerning the Rockwell C indentation adhesion test and the draft guidelines for the four point bending crack propagation method on one hand and on the crack spacing method on the other.

1 INTRODUCTION

1.1 Context of the research programme

Deposition of coatings as surface improvement is a well-established technology and is an extremely versatile means of adapting component performance to severe working conditions. It is used in a wide range of applications in all industrial sectors including the aerospace, automotive, engineering, construction, biomedical, optical and microelectronics industries.

An **urgent need for standardisation** in this important area is felt. Indeed, the relatively slow uptake of coating technology stems largely from a lack of end-user confidence in the quality of coatings supplied to them. This project deals with one important aspect of coatings that is essential to guarantee their properties, functional characteristics and performance, namely the **adhesion** between the coating and the substrate.

At present, adhesion of coatings is routinely tested in industry by two **engineering adhesion tests**: the scratch test and the Rockwell indentation test. These engineering adhesion test methods, **however, yield 'adhesion values' which depend not only on basic adhesion, *i.e.* the interfacial bond strength, but also on other factors**, which are related both to the test itself (scratching velocity, stylus geometry, etc.) and to other coating/substrate composite properties (hardness, roughness, coating thickness, etc.). Furthermore, only some of the observed failure events are related to detachment at the coating/substrate interface and are thus relevant as a measure of adhesion. Other failure events, such as **cohesive failure** within the coating or substrate may occur but clearly cannot be used to assess the coating/substrate adhesive strength.

Various attempts have been made to obtain a **direct quantitative measure of adhesion** which include, for example, laser pulse and ultra-centrifuge techniques, but these are either difficult to use or not completely devoid of ambiguity. Some work has already been carried out to develop a relatively simple and unambiguous quantitative adhesion test based on tensile testing which has given encouraging results.

1.2 Objectives

The main **objective** of this project was to obtain an increased understanding in the validity of the conventional engineering test methods for measuring adhesion. Therefore, results from the engineering methods are compared with results obtained by the novel quantitative tensile adhesion test. To this end, series of industrially relevant coatings with different properties have been produced with various levels of adhesion, by deliberately varying the substrate cleaning procedures and/or adhesion interlayer structure.

This study **results** in:
1) A better understanding of scratch test results, and resulting a revision of the ENV 1071-3:1994 'Determination of Adhesion by a Scratch Test'.
2) Increased knowledge concerning the Rockwell indentation method. A draft standard for an ENV is produced and submitted to CEN TC184/WG5.

3) Improved practical experience with the four point bending adhesion test and the tensile adhesion test. Guidelines for testing are prepared and submitted to CEN TC184/WG5 for consideration to adopt as an ENV.

1.3 Outline

This reports is divided in two main parts. The first part describes the methodology used in the set up of the tests. The selection of different types of coatings is presented and justified in the view of the adhesion tests. Thereafter, the various characterisation techniques for the coatings are enumerated and their principle and experimental set-up are briefly exposed. Finally, the theoretical principles of the four adhesion test under investigation and the used experimental set-ups are discussed in detail.

The second part of the report gives the results of the research program. According to the work program, the results of the deposition of the coatings (WP1), of the coating characterisation (WP2) and of the adhesion tests (WP3) are presented respectively.

The report is completed by the general conclusions and by some recommendations for future R&D.

The revised standard ENV 1071-3:1994 'Determination of Adhesion by a Scratch Test', the improved draft standard on indentation adhesion testing and the guidelines of test for the tensile test methods will be described in individual reports to be supplied by Vito, WTCM and ULB respectively.

2 METHODOLOGY

2.1 Selected coatings (WP1)

2.1.1 Substrates

Different types of substrates have been used depending on the coating to be deposited on it and the envisaged adhesion test.
For task WP1.2 (deposition of TiN) a ASP23 (1.3343) has been choosen.
The DLC coatings were deposited (task WP1.3) on DIN C60 as substrate material.
The electrodeposited Zn coatings (task 1.1) layed on a automotive steel.
In a later stadium of the project, the need was risen for some TiN and DLC coatings on automotive steel as well, to make the tensile adhesion test possible. More details on these exceptions are given in §3.1.1 and 3.1.2.
The dimension of the substrates was 30x30x5 mm^3 for the scratch test and the Rockwell indentation test and 120x20x15 mm^3 for the four-point bending test.
The substrates were numbered at one side, hardened, and polished at the other side (1 µm diamond finish).

2.1.2 Coatings

3 different types of coatings have been produced and tested:
- plasma assisted chemical vapour deposited diamond like carbon (PACVD DLC, Vito)
- physical vapour deposited titanium-nitride (PVD TiN, WTCM)
- electrodeposited zinc alloys (Zn, ULB)

These coatings have been chosen because of their industrial relevance and distinct mechanical properties. Typical literature hardness (H) and Young's modulus (E) values are: Zn (H = 0.7 GPa, E = 105 GPa), TiN (H = 25 GPa, E = 350 GPa) and DLC (H = 20 GPa, E = 150 GPa).

Three variants were produced by varying the deposition parameters for each coating material:
- variant A: standard coating with good adhesion.
- variant B: standard coating with poor adhesion.
- variant C: modified coating with good adhesion.

PACVD DLC (Vito – WP1.3)

This coating material combines high wear resistance with low friction, making it ideally suited for sliding wear applications such as bearings, gears and machine parts in general. The lifetime of the wear part is prolonged while at the same time the energy consumption of the machine is reduced. The industrial relevance of this material is generally acknowledged and it is expected that the market for DLC and related coatings will grow rapidly.

DLC coatings are produced by a capacitively coupled r.f. (13.56 MHz) PACVD process from CH_4 - H_2 precursors. The substrates are placed on the powered electrode which is subjected to an ion bombardment due to the negative self-bias, which develops as a

consequence of the difference in mobility between ions and electrons. The biasing conditions are controlled to produce coatings with optimum mechanical properties. The adhesion between the coating and the substrate is deliberately varied by changing the structure of a Si containing interlayer which is necessary to let a DLC layer adhere to an iron alloy. The coating thickness typically varies between 1 and 3 μm.

PVD TiN (WTCM – WP1.2)

Titanium-nitride coatings have found wide practice in industry because of their high wear resistance and good corrosion properties. Typical applications are protective coatings for metal machining tools, gears and dies as well as for esthetical purposes because of its golden colour.

The coatings are deposited in a Balzers industrial-size, PVD triode ion-plating equipment. The substrates are rotated in front of a Ti sputtering target under a nitrogen containing atmosphere. A DC substrate bias of -150 V is applied to the substrates to obtain TiN coatings with optimum mechanical properties. A typical high speed steel, such as for example DIN S-6-5-2 (WN 1.3343) is normally used as substrate material and the adhesion between the coating and the substrate is deliberately varied by changing the structure of the Ti adhesion interlayer. The coating thickness typically varies between 2 and 5 μm.

ELECTRODEPOSITED ZINC (ULB – WP1.1)

Zinc coatings and zinc alloy coatings (ZnFe, ZnNi, ZnMn, ZnCo, ...) are commonly used in industry for protecting steel against corrosion. Especially due to the increased use in the automotive industry, the production of electrogalvanised steel has become an important product output for steel producers.

These Zn alloy coatings are increasingly being produced by high current density electroplating of steel coils. Processes used on a large industrial scale require close control of current density and hydrodynamic conditions at the surface of the continuous steel sheet. Current densities ranging from 90 to 150 A/dm² and Reynolds numbers between 15 000 and 60 000 are currently achieved. Electrolytes are acidic, chloride or sulphate, without organic additives. They may be either highly acidic (pH < 1, up to 130 g/l H_2SO_4) or slightly acidic (pH ≈ 3.5). The thickness of the here deposited coatings vary typically between 10 and 20 μm. The adhesion between the coating and the substrate is deliberately varied by changing the electroplating parameters (the current density) and by modifying the steel surface preparation.

2.2 Characterisation: Experimental Set-up

Property	Technique	Partner
coating thickness	crater grinding	Vito
	cross section scanning electron microscopy	WTCM
surface roughness	laser profilometer	Vito
	contact profilometer	ULB, WTCM, Vito
composite hardness	macro-indentation	WTCM
coating hardness and Young's modulus	depth-sensing indentation	Vito
composition	electron probe microanalysis (EPMA)	Vito
	Auger spectroscopy (AES)	ULB
coating microstructure	cross section scanning electron microscopy	WTCM
residual strain preferential orientation	full X-ray diffraction (XRD) spectrum	ULB
DLC structure	Raman spectroscopy	Vito

We will shortly describe the principle and the experimental set-up of each of the characterisation techniques:

2.2.1 Crater grinding (coating thickness)

A spherical cap is ground into the coated specimen by rotating a ball, wetted by a suspension of diamond particles in ethanol, against that specimen. The test is stopped when the bottom of the crater has reached the substrate. The coating thickness t is calculated from the difference in diameter of the craters delimiting the outer coating surface and the interface between the coating and the substrate respectively.

This test is also called the Calo-test or the ball crater test.

Experimental (Vito):

A CSEM Calotest instrument was used to carry out the thickness measurements.

The ball, 30 mm in diameter, was made out of 100Cr6 bearing steel (ISO 3290), and the abrasive medium consisted of 1μm diamond paste suspended in ethanol, using a mixture of 1:4. The test is continued until the substrate is visible, and this typically takes a few minutes.

Five measurements per specimen were done.

2.2.2 Laser profilometer (surface roughness)

A light beam is focused on the surface. The roughness results in changes of the focus. There are advantages and limitations for each technique. The stylus may cause surface damage if the loading is too large. The lateral resolution is determined by the beam spot size, wavelength of light and by the resolution of the microscope lenses and other optical elements in the instrument.

Experimental (Vito):

An UBM ITF 100 A combined contact stylus - laser profilometer is used.

optical mode:	
wavelength:	780 nm;
beam spot diameter:	1 μm;
measurement range:	± 50 μm or ± 500 μm;
resolution:	< 0.01 % of range.

In each measurement mode, six measurements per specimen were done (3 measurements in two orthogonal directions, parallel with the specimen edges)

2.2.3 Contact profilometer (surface roughness)

This technique measures surface profiles with a diamond stylus probe that touches the surface. The main disadvantage of this technique is that the stylus may cause surface damage if the loading is too large. The lateral resolution of surface features depends on both the stylus radius and the slopes of the surface features being profiled. Measured surface roughness parameters may strongly depend on the lateral resolution of the profilometer.

Experimental (Vito, WTCM, ULB):

Vito: see above (2.2.2).
An UBM ITF 100 combined contact stylus - laser profilometer
contact mode:

diamond stylus tip radius:	5 μm;
stylus load:	0.7 mN;
measurement range:	± 100 μm;
vertical resolution:	1 nm.

WTCM: Perthen S8P profilometer.
A skidless pick-up with a stylus tip radius of 5 μm was used. The tracing force was 0.9 mN (approx.).

ULB: Dektak 3030 profilometer.
Tracing force = 0.1 mN, stylus tip radius = 12.5 μm.

2.2.4 Macro-indentation (composite hardness)

Experimental (WTCM):

The composite hardness was measured by a Hoytom 1003A Rockwell tester.

For a Rockwell C measurement a sphero-conical diamond indenter is used with a 120° deg angle with a spherical apex of 0.200 mm. A minimum load of 10 kg and a maximum load of 150 kg are used.

For Rockwell A measurements the same indenter is used. The major load in this case however is 60 kg.

2.2.5 Depth sensing indentation (coating hardness and Young's modulus)

In the depth sensing indentation (DSI) (also called nano-indentation) technique, load and indenter displacement are recorded in situ to obtain an indentation hysteresis curve. Not only the hardness but also the elastic (Young's) modulus can be derived from this curve. The resolutions of the method, typically 10 μN in load and 1 nm in displacement, allow the measurement of sub-micron surface mechanical properties. For thin surface coatings this is particularly important, to minimise the influence of the underlying substrate.
A typical curve is shown in §3.2.5.

Experimental (Vito):

The measurements were carried out using a NanoTest 550 instrument manufactured by Micro Materials Ltd. A trigonal pyramid (Berkovich) diamond indenter was used.

Analysis of the indentation curves was carried out following the method proposed by Oliver and Pharr [OLI 92]. A more elaborate description of the followed calculation method for the hardness and Young's modulus is given in the 12 month progress report of Vito in annexe A.

The test-parameters used were as follows:

Table 2.2-1: DSI test parameters.

max. depth	500 nm
initial load	0.05 mN
loading/unloading rate	1 mN/s
distance between indents	50 μm
drift acquisition time	30 s
hold time at max. load	10 s

Ten indents per specimen were performed, and outliers were rejected following ASTM Standard E 178-80. At least 5 measurements per specimen were used for the calculations.

2.2.6 Electron probe microanalysis (composition)

EPMA is a technique used to determine the elemental composition of a specimen by detecting characteristic X-rays generated in the specimen by interaction with an electron beam. The X-rays are analysed using a solid state detector according to their energy (EDXA: Energy Dispersive X-ray Analysis), or using diffraction crystals according to their wavelength (WDXA: Wavelength Dispersive X-ray Analysis). The latter method allows to analyse the characteristic X-ray spectrum with greater resolution.

Experimental (Vito):

Analytical apparatus: JEOL SUPERPROBE JXA-8621.
Off-line matrix correction software: STRATA v5.0.
Depending on the nature of the coatings, different electron beam voltages and currents were used. WDXA was chosen for all analyses.

Qualitative analyses, quantitative analyses and (elemental) line scans were applied to all the specimens in order to identify the elements present, to determine the composition and to check the homogeneity of the coatings, respectively.

2.2.7 Auger spectroscopy (composition)

Auger spectroscopy is used for compositional analyses in the surface layer of solid materials. The information depth from where Auger electrons are provided is typically 3 nm. Consequently, only the first atomic layers of the material can be investigated. This is particularly interesting for studying the oxidation or corrosion phenomena. Combined with ionic etching, depth profiling can be done. The composition of very shallow layers, like interface layers between substrate and coating can be determined by AES depth profiling. The elements H and He can not be detected by AES. Furthermore, the accuracy is rather low (± 30 % for quantitative analysis), except if a standard with a composition close to the sample is available.

2.2.8 Bending beam stress measurements

The presence of stresses in a coating on a thin substrate will cause the substrate to bend elastically. Measurement of the substrate bending is a common method for determining the stress in a coating. With the substrate touching the table, a concave surface indicates that the stresses in the coating are tensile, and vice versa. For a thin coating on a relatively thick substrate (thin film approximation [CHI 92]), the stress in the film, σ, can be calculated from the deflection of the free end of the strip, δ, using the simple Stoney equation:

$$\sigma = \left(\frac{E}{1-\nu}\right)_s \frac{t_s^2}{3L^2 t_c}\delta \qquad (2.2\text{-}1)$$

where $(E/1-\nu)_s$ is the biaxial modulus of the substrate, t_s and t_c are the thicknesses of the substrate and the coating, respectively, and L is the length of the strip. This equation is only applicable if the width-to-length ratio of the substrate is smaller than approx. 1/5.

Experimental:

Alkali zinc borosilicate glass strips (thickness code 0 = 85 to 130 µm) with dimensions of approx. 5 mm x 50 mm are used. The Young's modulus, E, Poisson's ratio, ν, and thermal expansion coefficient, α_{th}, for this material are 74.5 GPa, 0.22 and 7.4 10^{-6} /K, respectively. A thin coating (usually < 500 nm) of the material under investigation is deposited on the glass strip, to prevent breaking of the thin glass strip. To determine the deflection of the free end of the strip, it is taped at one end onto an optical flat, and the distance between the other end of the strip and the surface of the optical flat is measured using a eye-piece lupe with measuring scale.

2.2.9 XRD Stress measurements

X-ray diffraction offers an in situ observation of the elastic strain of the crystal lattice close to the surface of polycrystalline materials. The lattice strain is measured in several directions. The strain tensor, characteristic of the sampled material, can then be derived. From the strain tensor, the stress state can be calculated with the aid of elastic constants.

Experimental

Phase identification was done by a coupled θ-2θ measurement (Cu) on a Siemens D5000 machine in a Bragg-Brantano configuration. The measurement was done between 30° and 150° with step 0.02° (8 sec/step).

Stress measurements were done with an uncoupled θ-θ Philips diffraction apparatus with thin film attachment (Co). The stress measurements were based on a Reuss approach (constant stress).

Measurements for Zn were done by d-sin$^2\Psi$ method on the <112> plane. Step was 0.3° while the measuring time was variable (criterium: signal/noise ratio had to be at least 50). The diffraction slit was 0.25°.

The LIBAD method was used for the TiN measurements. The method is discussed in detail in [Ack 94]. The major aim of this method is to gain as much diffracted intensity from the coating as possible. Therefore, the X-ray beam enters the sample under a low angle α, let say between 0.6 and 5°. The angle α is fixed. However, the strain has to be measured in several directions of ψ. This is achieved in the LIBAD method by scanning the 2θ angle of several (*hkl*) planes instead of one single plane as in the d-sin$^2\psi$ method.With this method the incident angle is kept constant while all peaks are scanned.
The step and measuring time were chosen in such a way that a signal/noise ratio of at least 75 was reached. The diffraction slit was 0.25°. The incident angle was chosen in such a way that only the upper part (1 μm) of the coating was measured.

2.2.10 Raman spectroscopy (DLC structure)

Raman spectroscopy is an analytical technique that yields information about the molecular structure of materials. The specimen under investigation is being irradiated with a strong, monochromatic light source (focused laser beam). The radiation scattered by the specimen is analysed by means of a monochromator. The energy loss or gain of photons with respect to the incident radiation is equivalent to the difference between two vibrational energy states of Raman active molecules in the material under investigation.

Experimental:

A DILOR XY800 confocal macro Raman instrument was used.
Ar-laser wavelength: 514.5 nm;
laser spot diameter: 100 μm;
laser power: 100 mW;
gratings: 1800 mm^{-1};
wavenumber range: 450 - 2000 cm^{-1}.
Three scans per specimen were recorded.

2.3 Theoretical principles of adhesion tests

2.3.1 Scratch Adhesion Test

The conventional scratch test consists of drawing a diamond stylus across the surface under increasing normal load, until some well defined failure event is observed in a regular fashion along the scratch track (Fig. 2.3-1). The normal load at which this occurs is called the critical normal load L_c (unit: N). The failure event is determined by inspection of the scratch track under a microscope, after the scratch has been made. When the coating fails by spallation from the substrate, the corresponding critical load is considered to be relevant as a measure of adhesion.

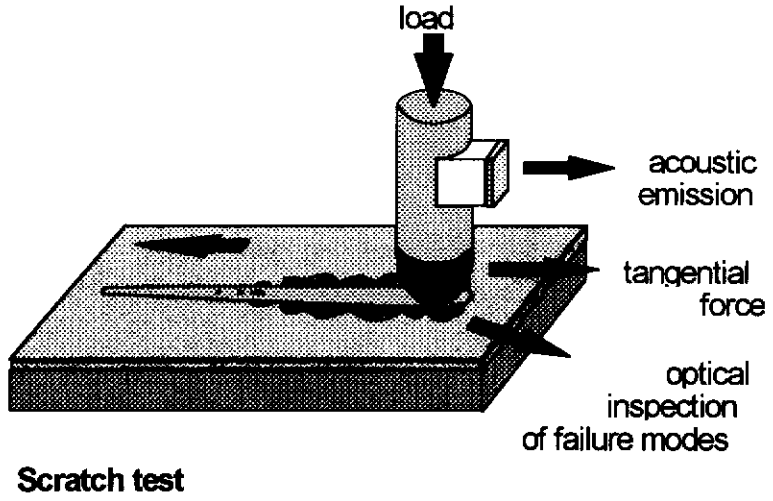

Fig. 2.3-1 Schematic representation of conventional progressive loading scratch test.

The scratch test method can be operated in the following 3 operation modes:

- **Single pass conventional progressive loading scratch test (SPST)**: by applying a load ramp to the scratch stylus during the displacement of the specimen underneath it.

- **Single pass operation at constant loads (CLST)**: by the stepwise increasing of the normal load between successive scratches carried out under constant load at different locations on the specimen surface.

- **Multipass operation at constant sub-critical load (MPST)**: by the repeated scratching under a constant sub-critical load within the same scratch track.

The SPST mode is used for the first order assessment of critical loads corresponding to major coating damage failure, while the CLST mode allows the statistical damage analysis of coatings along their surface. Finally, the MPST mode subjects the coated surface to a low-cycle fatigue type contact, which is considered to better simulate real working conditions of coated components. These three operation modes have been explored within the framework of this research programme.

For the first two modes, guidelines of test are described in the European pre-Standard ENV 1071-3:1994 'Determination of Adhesion by the Scratch Test'.

As for other engineering adhesion test methods, 'adhesion values' (critical loads) obtained by scratch testing depend not only on basic adhesion, *i.e.* the interfacial bond strength, but also on other coating/substrate composite properties (hardness, modulus, roughness, friction and coating thickness). As a consequence, the scratch test can at best be a semi-quantitative assessment of coating/substrate adhesion: if performed with care, the technique can repeatedly enable the ranking of the adhesion properties of a number of similar coating/substrate composites.

2.3.2 Rockwell Indentation Adhesion Test

In this test, the coated surface is indented with a diamond Rockwell C indenter causing damage to the coating close to the indent. The failure event is determined with a metallographic microscope (100x) and compared with the different failure classes shown in Fig. 2.3-2. This allows the coating/substrate adhesion to be classified from 'Adhesion Strength' AS1 to AS6.

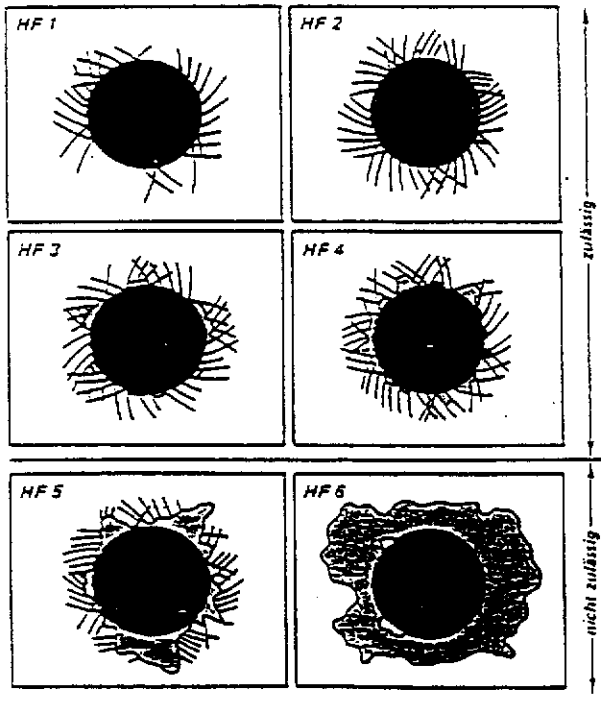

: **crack network;**
: **delamination**

Fig. 2.3-2 Adhesion classes with the Rockwell indentation test.

The indentation is being performed following the European Standard EN 10109-1:1995, but the Rockwell indentation adhesion test on its own has not yet been the subject of standardisation. Test guidelines have been described in VDI-Richtlinie 3198-1991 and DIN Fachbericht 39-1993, p. 213.

2.3.3 Four Point Bending Adhesion Test

Fig. 2.3-3 shows the design of the four-point bending test.

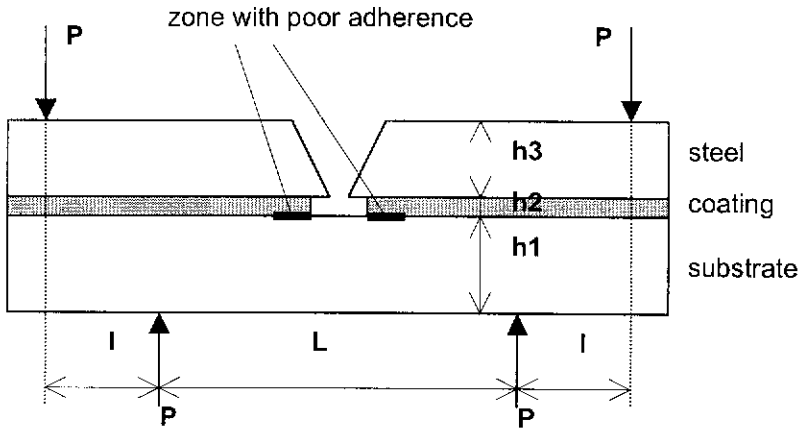

Fig. 2.3-3 Design of the four-point bending test.

Griffith's theory postulates that under a given loading, the crack is propagating if the total energy of the system decreases during the propagation. For an increase in crack size of dA, the crack will propagate if:

$$G_C\, dA \leq d(W - U_E) \tag{2.3-1}$$

with W= the potential energy of the external forces (Nm);
U_E= the stored elastic strain energy (Nm);
G_C= the critical energy release rate (N/m).

Under constant displacement:

$$\frac{(dW)_P}{dA} = 0 \tag{2.3-2}$$

P is the load (N). Equation 2.3-1 becomes now:

$$G_C = -\left(\frac{dU_E}{dA}\right)_P \tag{2.3-3}$$

For the crack located between the inner loading lines, the moment is constant. From the Euler-Bernouilli's beam theory, the stored elastic strain energy can be expressed in terms of applied moment M. G_C is given by equation 2.3-4.

$$G_C = \frac{M^2}{2B}\left(\frac{1}{E_1 I_1} - \frac{1}{(EI)_0}\right) \tag{2.3-4}$$

with M=P*l/2 (Nm);
E_1I_1= the flexional rigidity of the cracked beam (Nm^2);
$(EI)_0$= the flexional rigidity of the uncracked beam (Nm^2);
B = the width of the beam (m).
The flexional rigidity can be expressed analytically by:

$$(EI)_0 = E_1 I_1 + E_2 I_2 + E_3 I_3 + \frac{E_1 S_1 E_2 S_2 (h_1 + h_2)^2 + E_1 S_1 E_3 S_3 (h_1 + h_3)^2 + E_2 S_2 E_3 S_3 (h_2 + h_3)^2}{4(E_1 S_1 + E_2 S_2 + E_3 S_3)} + E_1 E_2 h_1 h_2 h_3 \frac{S_1 + S_2 + S_3}{E_1 h_1 + E_2 h_2 + E_3 h_3} \tag{2.3-5}$$

$$E_1 I_1 = E_1 \frac{B h_1^3}{12}$$

In plane strain conditions, the apparent modulus is larger and is given by:

$$E_{app} = \frac{E}{1 - \nu^2} \tag{2.3-6}$$

2.3.4 Tensile Adhesion Test

2.3.4.1 principle

The coated sample is subjected to an increasing tensile strain, causing the film to crack and break into segments as illustrated in Fig. 2.3-4.

Fig. 2.3-4 Schematic representation of the tensile test for multiple crack spacing.

Cracks are nucleated perpendicular to the tensile axis, x_1, and change the stresses and strains in the neighbourhood. Shear stresses are developed in the vicinity of the interface, resulting from the difference in the axial displacement between the coating and the substrate (Fig. 2.3-5):

$$\tau(x_1) = 2\mu\gamma(x_1) \tag{2.3-7}$$

$$\gamma(x_1) = \frac{u_c(x_1) - u_s(x_1)}{g} \tag{2.3-8}$$

with μ is the shear modulus of the interface,
(x_1) the shear strain at the interface,
$u_c(x_1)$ and $u_s(x_1)$ are the deformations in the coating and the substrate respectively,
g is a characteristic length of the interface,
x_1 is the co-ordinate along the interface with origin at the crack.

From the local force balance, a differential equation for the stress in the coating is developed:

$$\frac{d\sigma(x_1)}{dx_1} = \frac{1}{h}\tau(x_1) \tag{2.3-9}$$

where h is the coating thickness; the tensile stress is assumed uniform through the thickness of the coating.

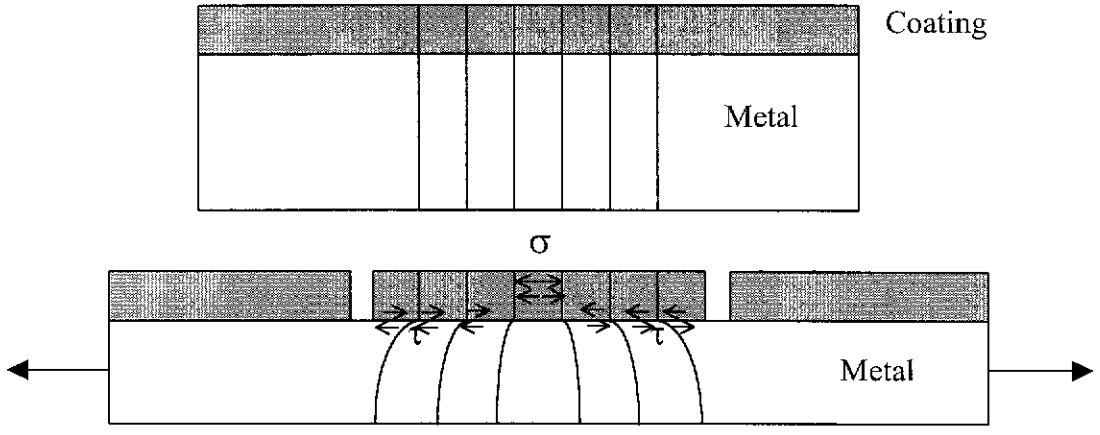

Fig. 2.3-5 Load transfer between metal and coating resulting from the difference in the axial displacement between the coating and the substrate.

The maximum shear stress, τ_{max}, at the interface is obtained as:

$$\tau_{max} = \frac{kh\sigma_f}{\lambda_{max}} \tag{2.3-10}$$

with λ_{max} is the maximum crack spacing,
σ_f is the tensile strength of the film
k depends on the shear stress distribution along the interface, for which different models exist shown in next paragraph.

2.3.4.2 Models

Different forms have been assumed for the shear stress distribution $\tau(x_1)$, as illustrated in Fig. 2.3-6. Table 2.3-1 gives the values of k calculated for the different distributions and to be used in equation 2.3-10.

Table 2.3-1 The integration constant, k, for different shear stress distribution.

Reference	k
Tyson and Davies [TYS 65]	6
Kelly [KEL 66]	2
Agrawal and Raj [AGR 89]	π
Shieu [SHI 90]	π

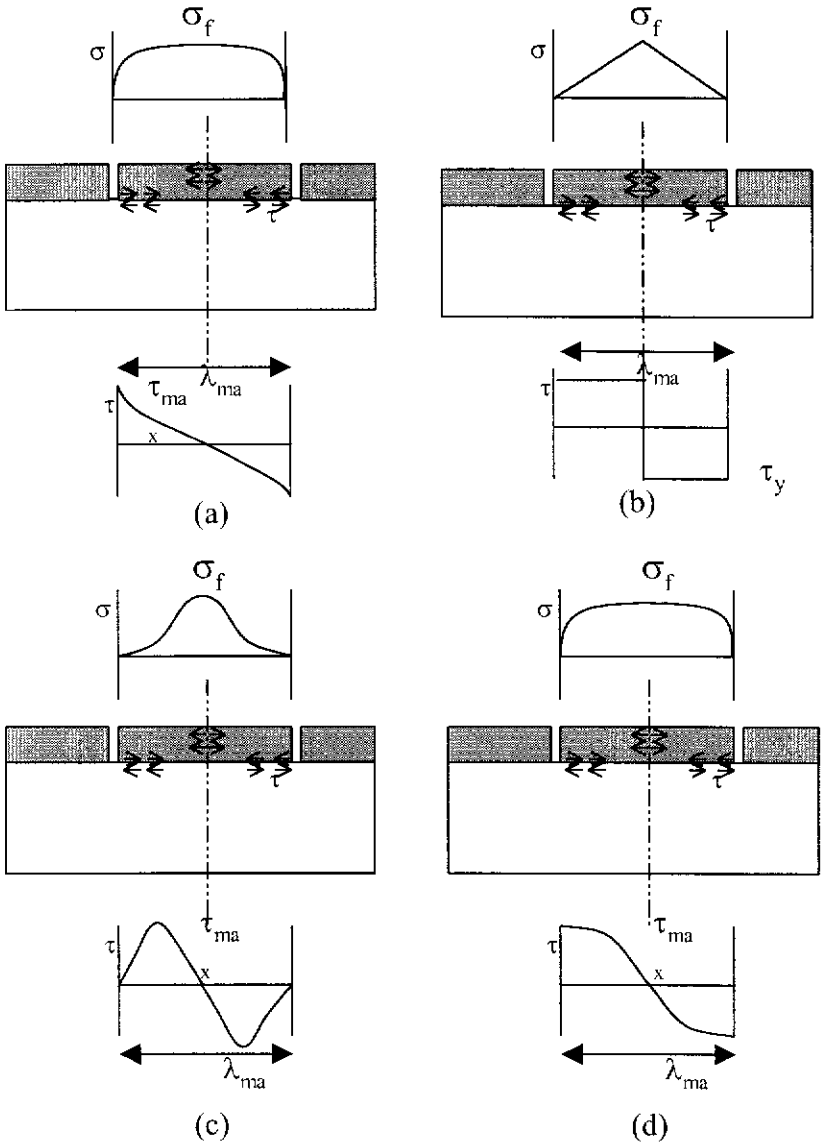

Fig. 2.3-6 Different models of the shear stress distribution along the interface between the metal and the coating, according to (a) Tyson and Davies (b) Kelly, (c) Agrawal and Raj, (d) Shieu.

2.3.4.3 Crack density distribution

The expected dependence of the crack spacing on the imposed strain is depicted in Fig. 2.3-7.

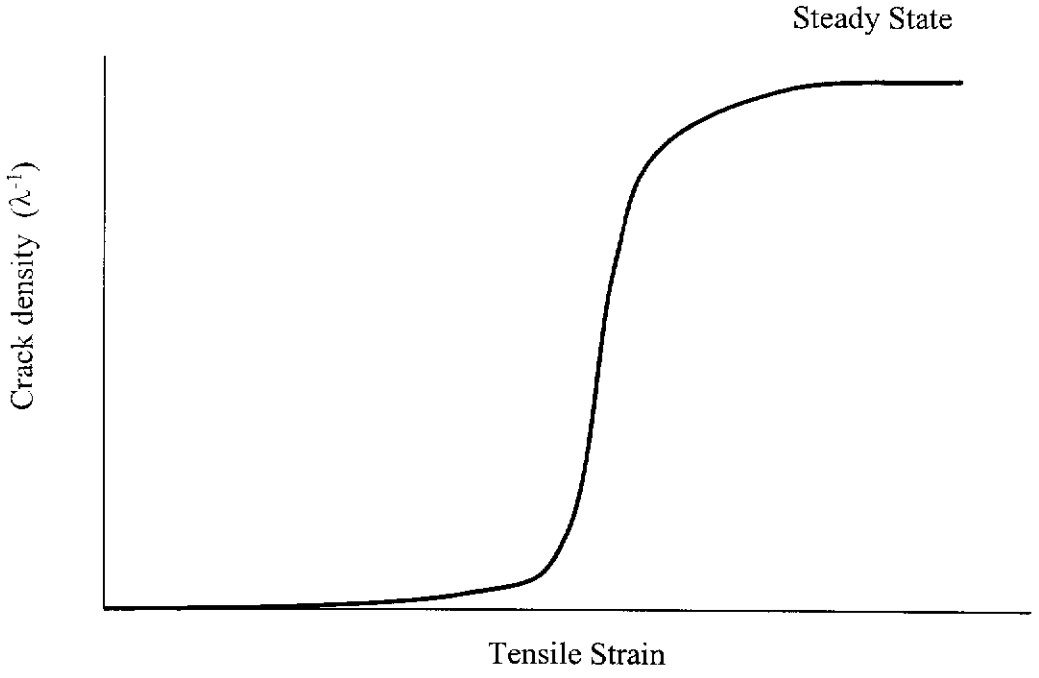

Fig. 2.3-7 Shematic plot of crack density as a function of imposed tensile strain.

The strain at which the cracks begin to appear, ε_f, gives a measure of the tensile fracture strength of the film.

$$\sigma_f = E_f * \varepsilon_f \tag{2.3-11}$$

Any residual stress initially stored in the coating should be added to the right-hand side of this equation.

In practice, the cracks will not be evenly spaced but have a statistical distribution due the brittle nature of the coatings . Even if the strength of the film were uniform everywhere, a spread of spacing covering a factor of two would be expected, from λ_{max} to $\lambda_{max}/2$. This factor reflects the extremes of a particular section of film either just breaking into two or just failing to do so. In fact, fracture of brittle materials is characterised by a strength distribution $F(\sigma)$ representing the fraction of failed specimens under loading σ [FRE 68]. For coating materials this function is obtained as a Weibull function.

$$F(\sigma) = 1 - \exp\left\{-\left(\frac{\sigma + \sigma^i - \sigma_f^0}{\sigma_f}\right)^m\right\} \tag{2.3-12}$$

$$F(\sigma) = 1 - \exp\left\{-\left(\frac{\sigma - \sigma_{th}}{\sigma_f}\right)^m\right\} \tag{2.3-13}$$

where $\sigma_{th}=\sigma_f^{\circ}-\sigma^i$ is the threshold value of fracture, σ_f° and σ_f are the lower limit and the mean value of the strength, σ^i is the residual or internal stress and m, the Weibull modulus. The higher the value of m, the more homogeneous are the mechanical properties in the volume of the coating.

Ramsey et al. [RAM 91] as well as Henstenberg [HEN 89] used Monte Carlo simulations to determine the crack spacing distribution for a given value of the Weibull modulus, m, assuming interface sliding at a constant shear stress, governed by the shear yield stress of the metal, τ_y (Kelly model [KEL 66]). For example, the Monte Carlo simulations of Henstenberg [HEN 89] are showed in Fig. 2.3-8.

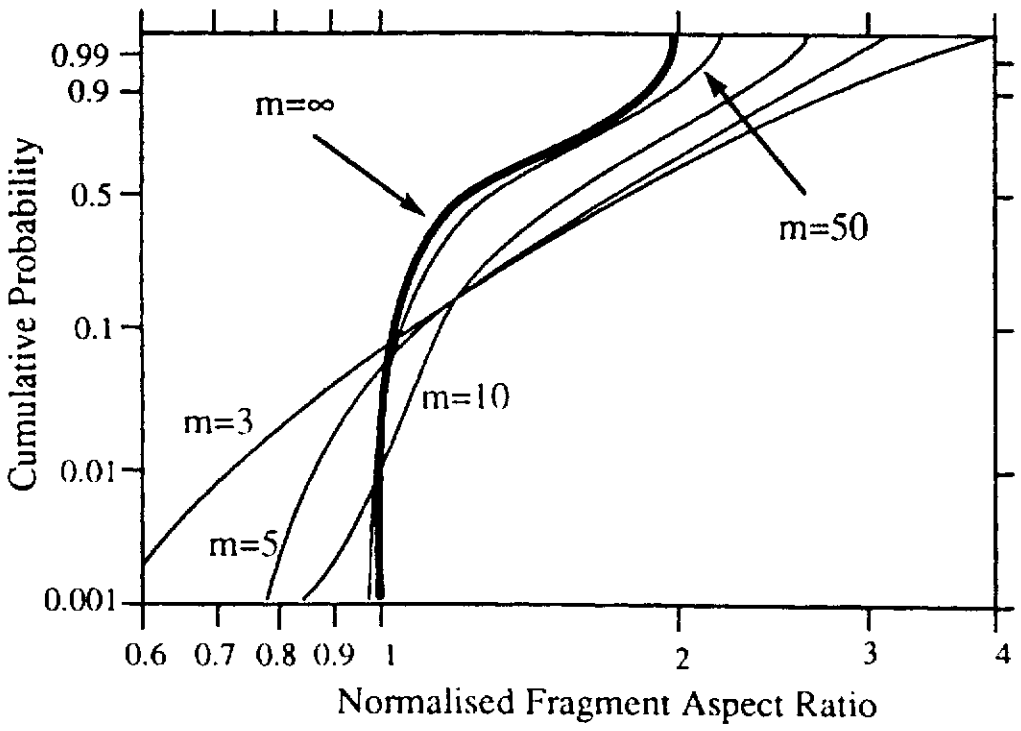

Fig. 2.3-8 Probability distribution functions for the aspect ratio of fragments, with several values of the Weibull modulus m, according to the Monte Carlo model of Henstenberg and Phoenix.

2.3.4.4 Film Decohesion

In some systems, film cracking may be accompanied by interface decohesion. Interface crack propagation is governed by the associated energy release rate, G_d.
Once nucleated, the non-dimensional energy release rate initially diminishes with crack propagation length.
Fig. 2.3-9 illustrates the evolution of the energy release rate related to film decohesion as a function of the non-dimensional crack length. The increase in decohesion length with load may be used in conjunction with Fig. 2.3-9 [HU 89] to estimate the energy release rate G_d.

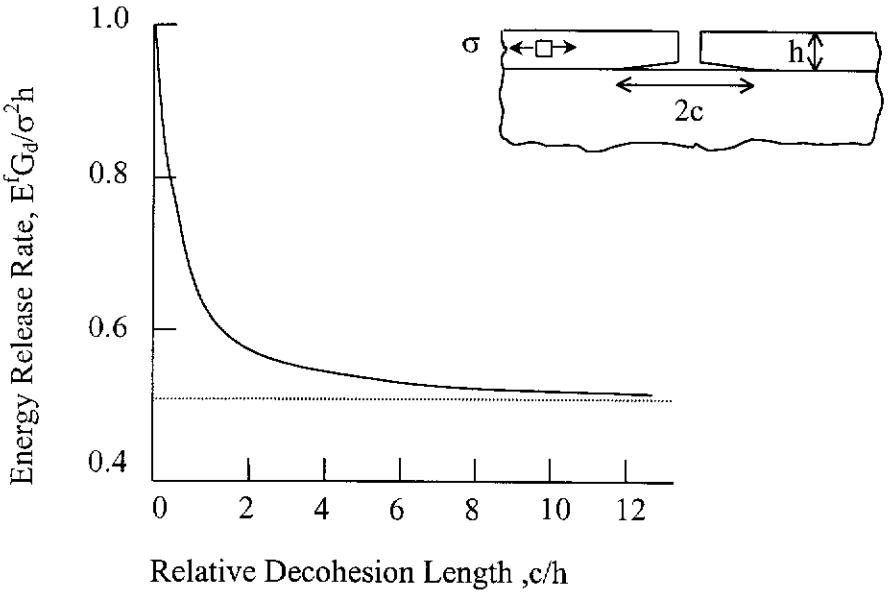

Fig. 2.3-9 Variations in the non-dimensional energy release rate with decohesion length for plane strain film decohesion in an elastically isotropic system.

Steady state condition develop for c/h>5 with a phase angle of loading, $\Psi \cong 52°$ [Bow 73]. Then, the energy release rate may be evaluated as [Suo 89],[Gil 84]:

$$G_d = \frac{1-\nu^2}{2E_f} * \sigma_d^2 * h \qquad (2.3\text{-}14)$$

This relation is only true if the crack front at the interface is long and if debonding does not interact with existing cracks.

In practice however, a scatter in the local properties leads to debonded regions of limited size and equation 2.3-14 and cannot be used to describe delamination in this simple form. Therefore, it is useful to estimate a threshold strain $\varepsilon_{th,d} = \varepsilon_d^\circ - \varepsilon_i$ for delamination as a measure of the material parameter ε_d°, a lower limit of the delamination strain. ε_i is the internal strain in the coating. The steady state delamination strain ε_d° may be related to the lower limit of the bonding energy γ by [Gil 83]:

$$\gamma = \frac{E_f}{2(1-\nu^2)} (\varepsilon_d^0)^2 h \qquad (2.3\text{-}15)$$

Voronkin and al. [Vor 93] studied cracking and decohesion of amorphous hydrogenated carbon films on polymeric substrate by tensile testing. They suggest that a ratio of the area of fracture across the substrate to the whole film area should be used for quantitative estimation of adhesion:

$$A = \frac{S_1 - S_2}{S_1} \qquad (2.3\text{-}16)$$

where S_1 is the mean width of the film fragment and S_2 is the mean size of the zone in which the delamination occurs at the film-substrate interface.

2.3.4.5 Applicability

To be valid, the test implies that the substrate deforms under stress with a greater displacement than the coating. The coating has therefore to be more brittle than the substrate. In the framework of this project, the test is used for TiN and DLC coatings on deformable automotive steel. The method was not applicable to hard steel substrates: the deformation of the substrate was too low to initiate cracks.